Electronic Supplementary Material (ESI) for ChemComm.

3R Phase of MoS_2 and WS_2 Outperforms Corresponding 2H Phase for Hydrogen Evolution

Rou Jun Toh,[a] Zdeněk Sofer,[b] Jan Luxa,[b] David Sedmidubský,[b] and Martin Pumera*[a]

[a]Division of Chemistry & Biological Chemistry, School of Physical and Mathematical Sciences, Nanyang Technological University, Singapore 637371, Singapore and

[b]Department of Inorganic Chemistry, University of Chemistry and Technology Prague, Technická 5, 166 28 Prague 6, Czech Republic

*Corresponding author: email address: pumera.research@gmail.com

Experimental

Materials. WO_3 (99.9%) and MoO_3 (99.9%) were obtained from Sigma-Aldrich, Czech Republic. 2H-MoS_2 (AA) and 2H-WS_2 (AA) were purchased from Alfa Aesar, Czech Republic. 2H-MoS_2 (SA) and 2H-WS_2 (SA) were purchased from Sigma Aldrich, Czech Republic. Sulphuric acid was purchased from Sigma Aldrich, Singapore. K_2CO_3 (>99%), S (>99%) and toluene were obtained from PENTA, Czech Republic. Glassy carbon (GC), the Ag/AgCl reference and Pt counter electrodes were acquired from Autolab (The Netherlands). 2H-MoS_2 single crystals originate from Sörumsaasen mine, Spikkestad, Drammen, Norway. 2H-WS_2 single crystals were prepared by vapour transport method using 2 g of WS_2 and 0.2 g of iodine in quartz glass ampoule (200x20 mm). The thermal transport growth of 2H-WS_2 crystals was performed with thermal gradient between 950 °C and 900 °C for two weeks.

Instrumentation. X-ray diffraction (XRD) was done with a Bruker D8 Discoverer diffractometer in Bragg–Brentano parafocusing geometry. A Cu K_α radiation was used. Diffraction pattern were collected between 10° and 80° of 2θ. The obtained data were evaluated using HighScore Plus 3.0e software. High resolution transmission electron microscopy (HR-TEM) was performed using an EFTEM Jeol 2200 FS microscope (Jeol, Japan). A 200 keV acceleration voltage was used for measurement. Sample preparation was attained by drop casting the suspension (1 mg mL^{-1} in water) on a TEM grid (Cu; 200 mesh; Formvar/carbon) and drying at 60 °C for 12 h. X-ray fluorescence (XRF) analysis was performed by ARL PERFORM'X sequential WD-XRF spectrometer equipped with an Rh anode end-window X-ray tube type 4GN fitted with 50 µm Be window. All peak intensity data were collected by software Oxsas in vacuum. The generator settings-collimator-crystal-detector combinations were optimized for all 82 measured elements with analysis time of 6s per element. The obtained data were evaluated by standardless software Uniquant 5 integrated in Oxsas. The analyzed powders were pressed into pellets about 5 mm thick and diameter of 40 mm without any binding agent and covered with 4 µm supporting polypropylene (PP) film. Scanning electron microscopy (SEM) was performed using a Jeol 7600F SEM instrument (Jeol, Japan) operating at 5 kV. Energy-dispersive X-ray spectroscopy (EDS) data were acquired on a Jeol 7600F instrument (Jeol, Japan) at 15 kV. X-ray photoelectron spectroscopy (XPS) measurements were performed using a Phoibos 100 spectrometer and a monochromatic Mg X-ray radiation source (SPECS, Germany). Survey (wide-scan) and high resolution spectra were recorded for each sample. For SEM, EDS, and XPS measurements, samples were prepared by coating a uniform layer of the materials under study onto carbon conductive tape. All voltammetric experiments were carried out using a µAutolab type III electrochemical analyser (Eco Chemie, The Netherlands) connected to a computer and controlled by the NOVA, Version 1.8.17, software. Electrochemical experiments were conducted in an electrochemical cell (5 mL) at room temperature. A three-electrode setup was employed. A platinum electrode served as the auxiliary electrode, an Ag/AgCl electrode functioned as the reference electrode and a glassy carbon (GC, 3 mm diameter) electrode was employed as the working electrode.

Phase composition calculations. For the basic estimation of 3R and 2H phase composition was used software HighScore Plus 3.0e, which automatically calculate phase composition based on diffraction pattern intensity. This method give 3R/2H ratio about 1:1 for all samples. Detail analysis of 3R/2H phase ratio was performed using Topaz software from Bruker based on Rietveld refinement method. The obtained 3R:2H ratio was in the range of 2.1:1 to 2.8:1. The structure models of MoS_2 and WS_2 for the respective 2H ($P6_3/mmc$) and 3R (R3mH) polymorphs were taken from Inorganic Crystal Structure Database, data entries 49801 and 38401 for MoS_2 and 651387 and 202367 for WS_2. All structure parameters except for lattice parameters were kept constant. The peak profiles were described in terms of fundamental parameter approach to model the instrument function for divergent beam geometry. Since the reflections exhibited a variable peak broadening due to different nanosizing effects in different crystallographic directions, a phenomenological Stephens model was applied for anisotropic peak broadening.[1] Moreover, a preferential orientation for (00l) and (110) direction was considered for 2H and 3R, respectively.

Procedures. *Synthesis of 3R phase MoS_2.* A mixture of K_2CO_3 (15 g), S (31 g) and MoO_3 (21 g) was heated at temperatures of 550 °C, 650°C or 750 °C. The heating was performed for 8 h in quartz glass tube loosely capped with quartz lid. The heating and cooling rate was 5 °C min^{-1}. Synthesized MoS_2 was leached with hot water and unreacted sulfur was extracted with toluene using Soxhlet extractor. Finally, the product was ultrasonicated with hot water and separated by suction filtration.

Synthesis of 3R phase WS_2. A mixture of K_2CO_3 (15 g), S (41 g) and WO_3 (33 g) was heated at temperatures of 550 °C, 650°C or 750 °C. The heating was performed for 8 h in quartz glass tube loosely capped with quartz lid. The heating and cooling rate was 5 °C min^{-1}. Synthesized WS_2 was leached with hot water and unreacted sulfur was extracted with toluene using Soxhlet extractor. Finally, the product was ultrasonicated with hot water and separated by suction filtration.

Hydrogen Evolution Reaction (HER) Studies on 2H and 3R Phase Transition Metal Dichalcogenides. Hydrogen evolution reaction (HER) efficiency of TMD materials were performed on glassy carbon (GC) electrodes. GC electrodes were first renewed using a 0.05 µm alumina particle slurry on a polishing pad and washing with ultrapure water. Subsequently, 1 mg mL^{-1} suspensions of TMD materials were prepared in ultrapure water and ultrasonicated for a period of 10 min prior to each electrochemical measurement to ensure homogeneity of the material under study. An aliquot (4 µL) was deposited on the electrode surface and left to dry at room temperature to yield a randomly distributed film of 4.0 µg of desired material on the GC electrode surface. The materials of interest include 2H-MoS_2 (AA), 2H-MoS_2 (SA), 3R-MoS_2 (550 °C), 3R-MoS_2 (650 °C), 3R-MoS_2 (750 °C), 2H-WS_2 (AA), 2H-WS_2 (SA), 3R-WS_2 (550 °C), 3R-WS_2 (650 °C) and 3R-WS_2 (750 °C). HER measurements were carried out using linear sweep voltammetry at a scan rate of 2 mV s^{-1} in a H_2SO_4 electrolyte (0.5 M). Linear sweep voltammograms were represented versus reversible hydrogen electrode (RHE). The measured potentials are calculated using the equation $E_{RHE} = E_{Ag/AgCl} + 0.059 \times pH + E^0_{Ag/AgCl}$, where $E_{Ag/AgCl}$ is the measured potential, pH of H_2SO_4 (0.5 M) given as zero, and $E^0_{Ag/AgCl}$ is the standard potential of Ag/AgCl (1M KCl) at 25 °C which is determined as 0.235 V.

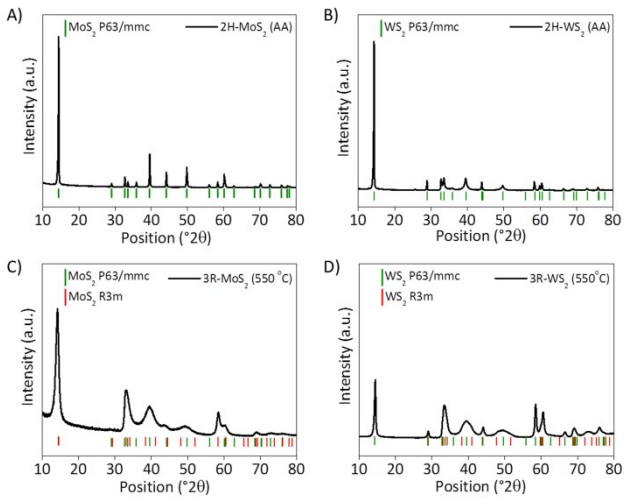

Figure S1. X-ray diffraction (XRD) patterns of A) 2H-MoS_2 (AA), B) 2H-WS_2 (AA), C) 3R-MoS_2 (550˚C), and D) 3R-WS_2 (550˚C).

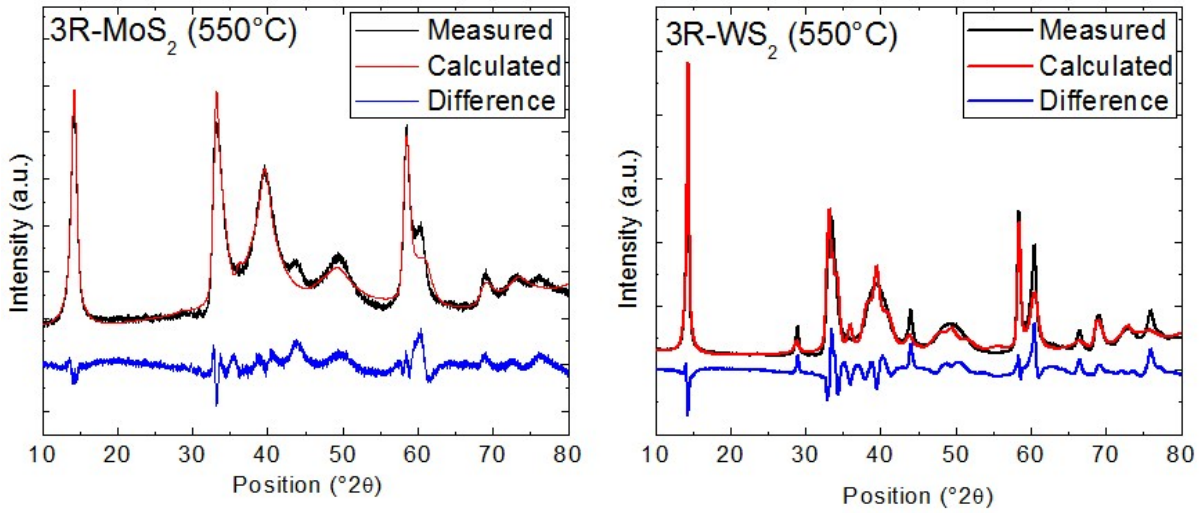

Figure S2. X-ray diffractograms with Rietveld method calculated profile and difference curve for samples 3R-MoS_2 (550°C) and 3R-WS_2 (550 °C).

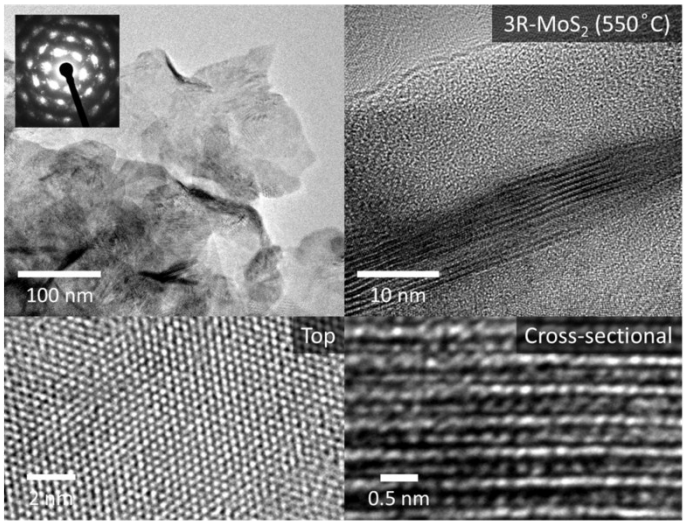

Figure S3. Transmission electron microscopy (TEM) image of 3R-MoS_2 (550˚C) sheets with corresponding selective area electron diffraction (SEAD) pattern High resolution TEM images show the top and cross-sectional views of 3R-MoS_2 (550˚C), indicating the desired 3R stacking of the atomic layers. Scale bars represent 80 nm, 10 nm, 2 nm and 0.5 nm respectively.

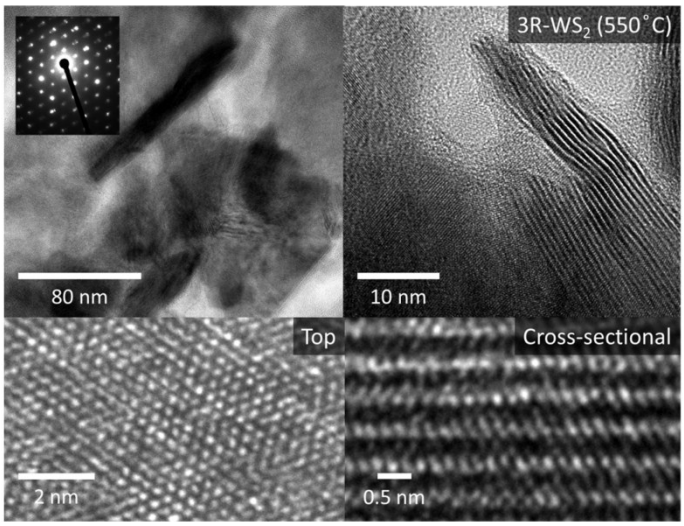

Figure S4. Transmission electron microscopy (TEM) image of 3R-WS_2 (550˚C) sheets with corresponding selective area electron diffraction (SEAD) pattern High resolution TEM images show the top and cross-sectional views of 3R-WS_2 (550˚C)), indicating the desired 3R stacking of the atomic layers. Scale bars represent 100 nm, 10 nm, 2 nm and 0.5 nm respectively.

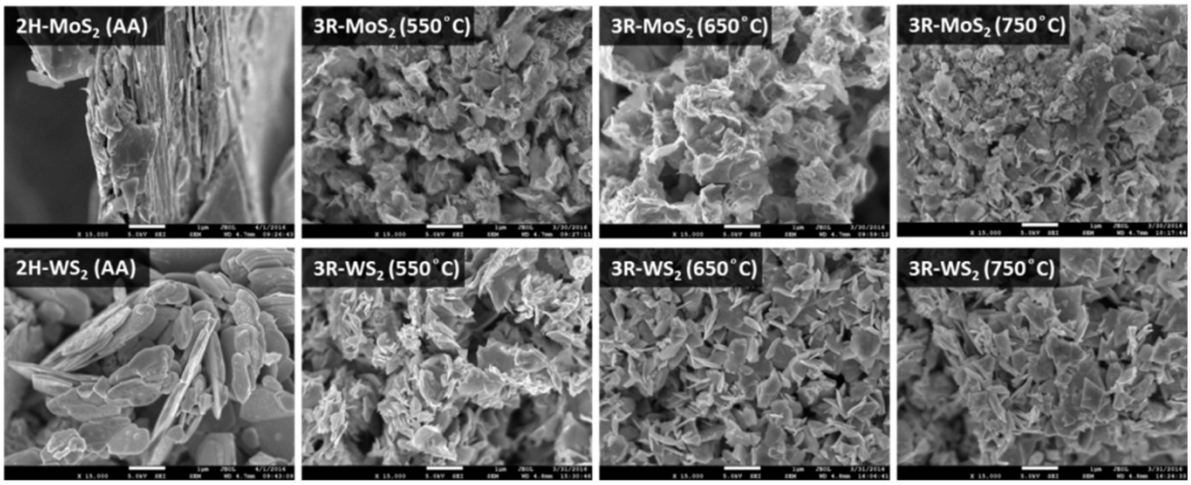

Figure S5. Scanning electron microscopy (SEM) images of the transition metal dichalcogenides; 2H-MoS_2 (AA), 3R-MoS_2 (550˚C), 3R-MoS_2 (650˚C), 3R-MoS_2 (750˚C), 2H-WS_2 (AA), 3R-WS_2 (550˚C), 3R-WS_2 (650˚C) and 3R-WS_2 (750˚C). Scale bars, 1 μm.

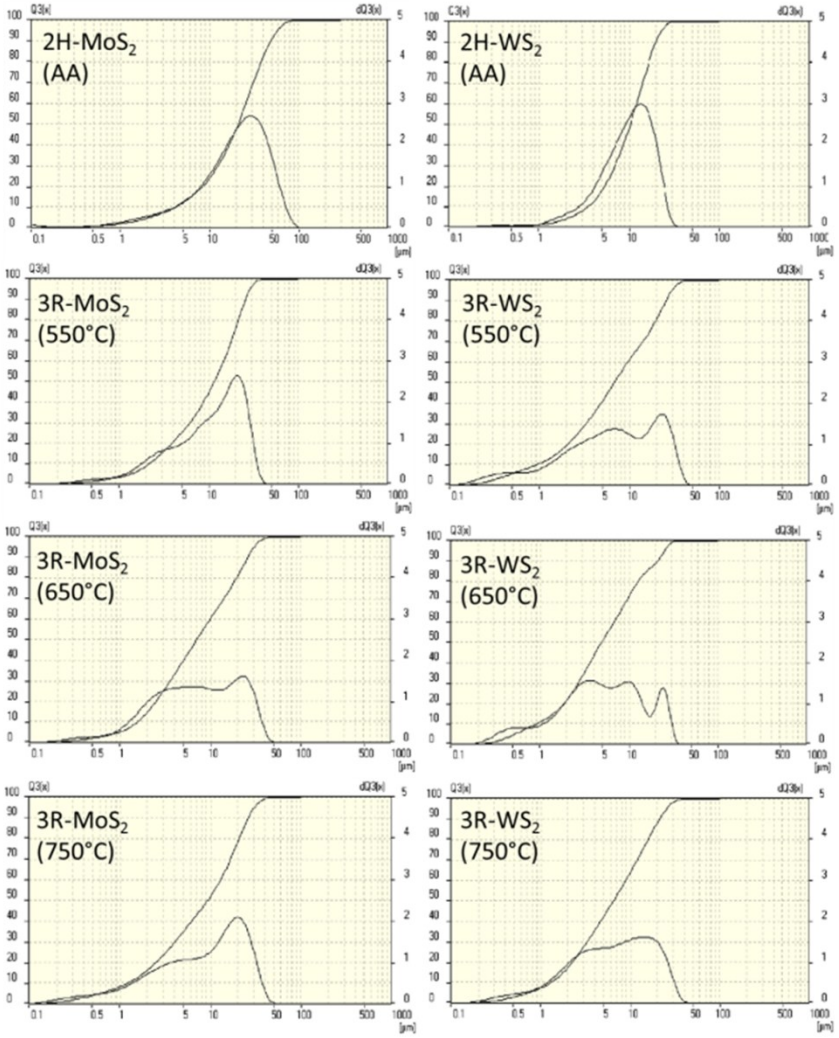

Figure S6. Particle size distributions of 2H-MoS_2 (AA), 3R-MoS_2 (550˚C), 3R-MoS_2 (650˚C), 3R-MoS_2 (750˚C), 2H-WS_2 (AA), 3R-WS_2 (550˚C), 3R-WS_2 (650˚C) and 3R-WS_2 (750˚C).

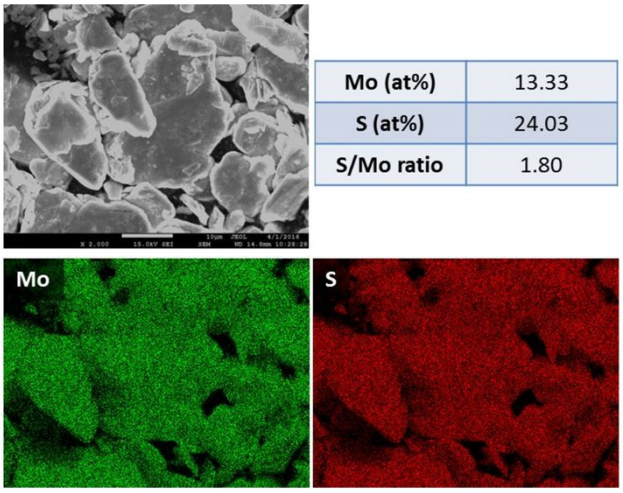

Figure S7. Energy-dispersive X-ray spectroscopy (EDS) data for 2H-MoS_2 (AA). Scale bar, 10 µm.

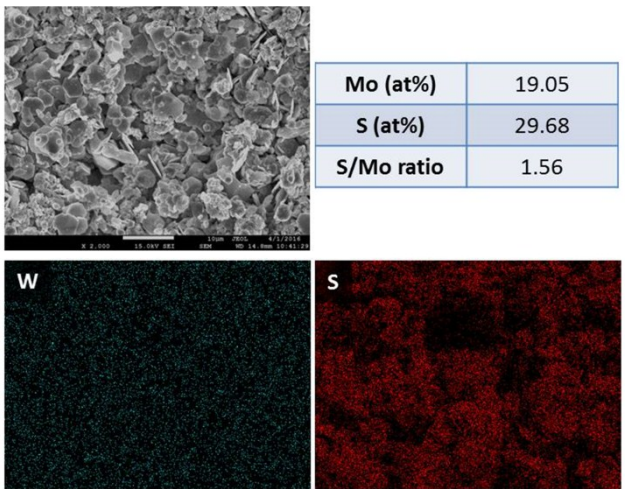

Figure S8. Energy-dispersive X-ray spectroscopy (EDX) data for 2H-WS_2 (AA). Scale bar, 10 µm.

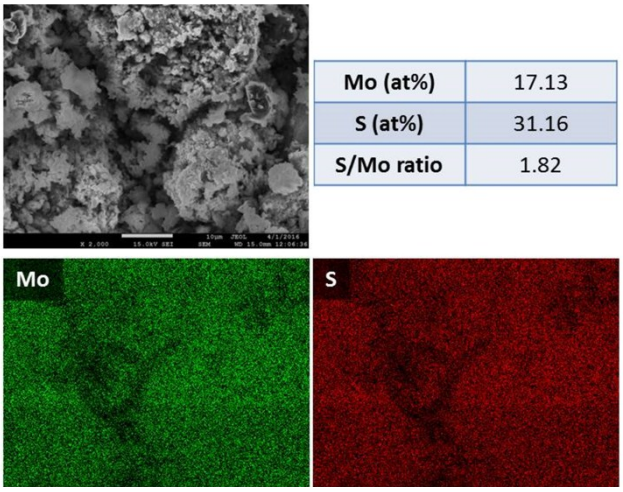

Figure S9. Energy-dispersive X-ray spectroscopy (EDS) data for 3R-MoS_2 (550˚C). Scale bar, 10 µm.

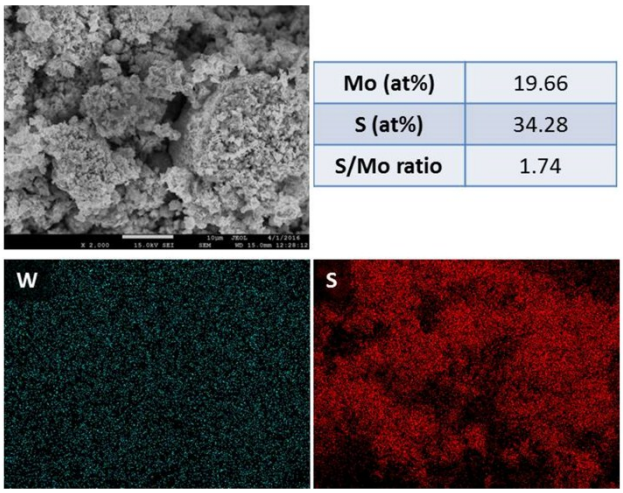

Figure S10. Energy-dispersive X-ray spectroscopy (EDS) data for 3R-WS_2 (550˚C). Scale bar, 10 µm.

Table S1. X-ray fluorescence analysis (XRF) of materials; elemental composition of Mo, W, S and K represented in weight percentage (wt.%). Concentration of all other elements are below 0.01 wt.%.

	Mo (wt%)	W (wt%)	S (wt%)	K (wt%)	Zn (wt%)	Fe (wt%)
3R-MoS_2 (550˚C)	59.18	0	39.61	1.19	0.012	0
3R-MoS_2 (650˚C)	53.62	0.012	45.76	0.592	0.012	0
3R-MoS_2 (750˚C)	60.14	0	39.68	0.162	0.014	0
3R-WS_2 (550˚C)	0.149	68.25	30.45	1.04	0	0.018
3R-WS_2 (650˚C)	0.169	68.06	31.15	0.598	0	0.018
3R-WS_2 (750˚C)	0.387	70.08	29.46	0.053	0	0.011

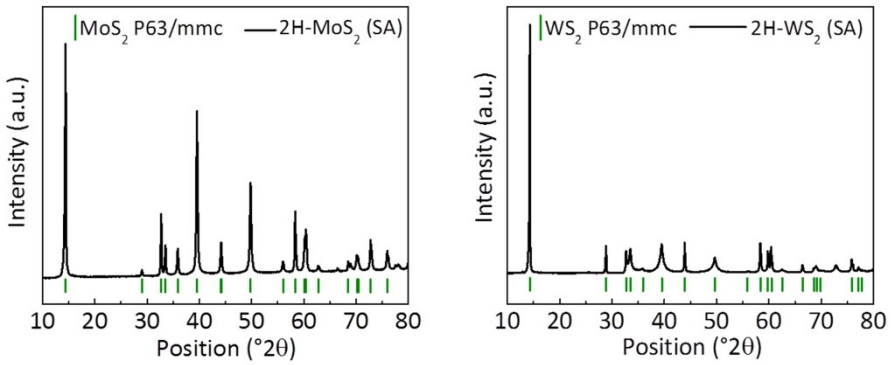

Figure S11. X-ray diffraction spectra of 2H-MoS_2 (SA) and 2H-WS_2 (SA).

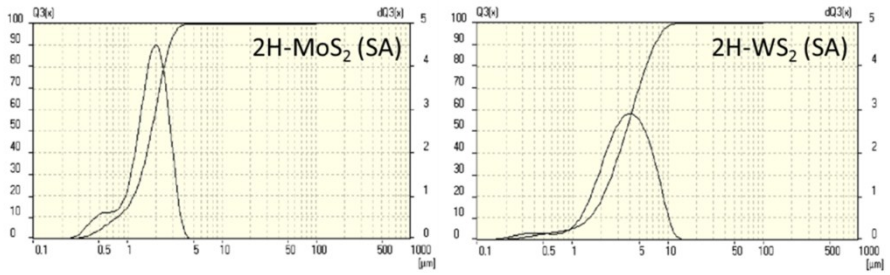

Figure S12. Particle size distributions of 2H-MoS_2 (SA) and 2H-WS_2 (SA).

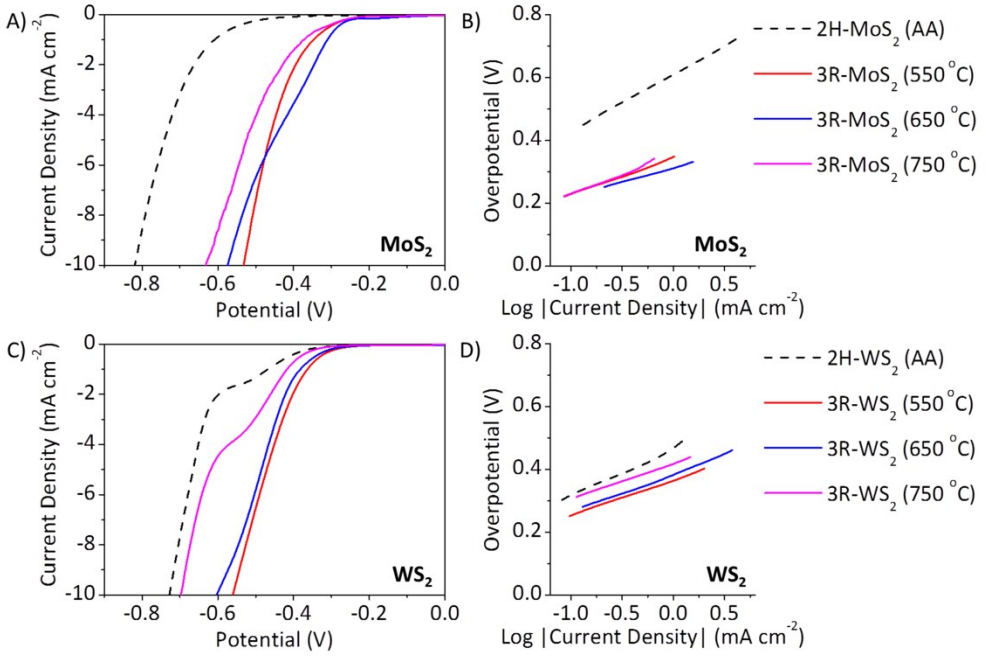

Figure S13. HER polarization curves of 2H and 3R phase TMDs. Linear sweep voltammograms for HER in acidic electrolyte on A) MoS_2 and C) WS_2 compounds. Tafel plots for B) MoS_2 and D) WS_2 compounds. Conditions: background electrolyte, H_2SO_4 (0.5 M); scan rate, 2 mV s^{-1}. All measurements were performed relative to the Ag/AgCl reference electrode and are corrected to reversible hydrogen electrode (RHE) potentials.

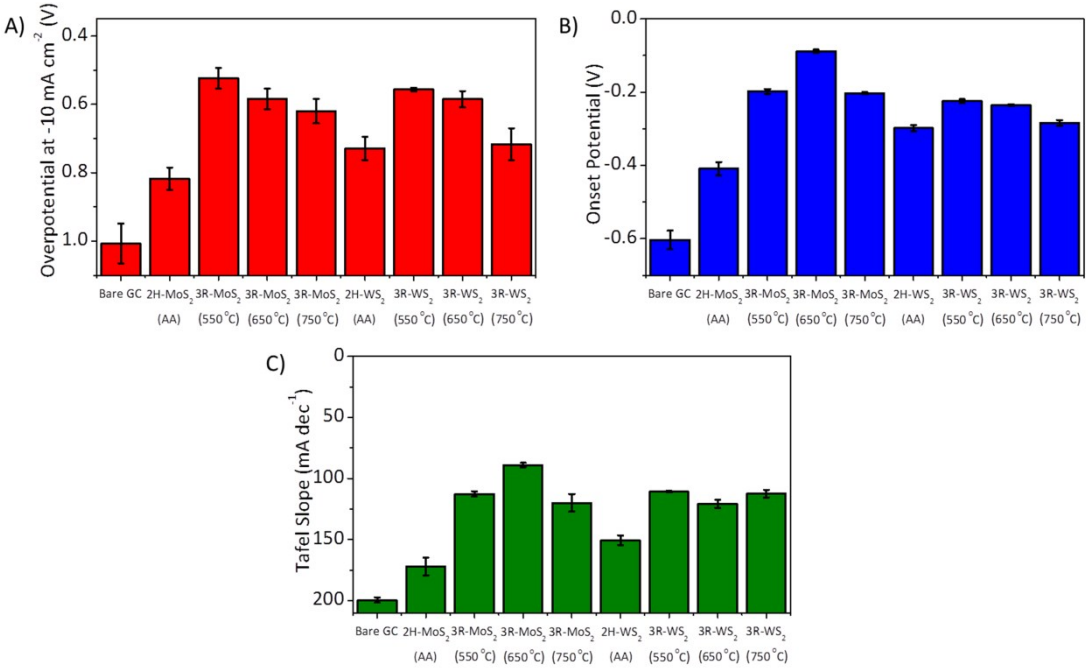

Figure S14. HER performance indices of all materials. Bar charts illustrate the averages of the A) overpotential at -10 mA cm^{-2} current density, B) HER onset potential and C) Tafel slopes for bare glassy carbon, MoS_2 and WS_2 in 2H and 3R phases; 3R phase MoS_2 and WS_2 were prepared at 550˚C, 650˚C or 750˚C.

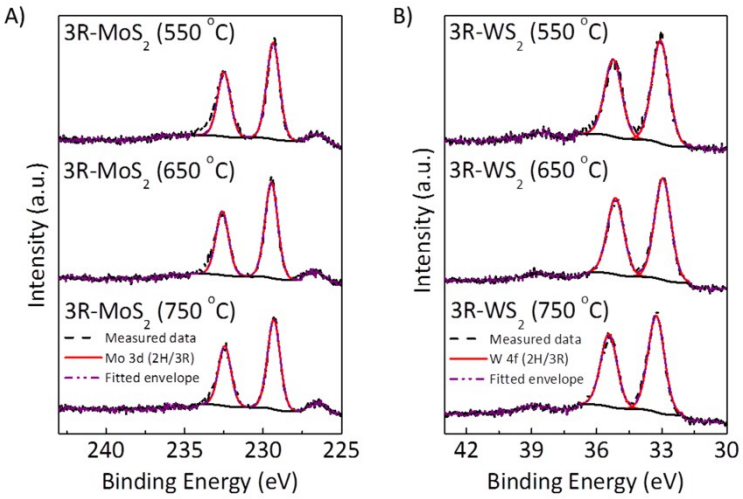

Figure S15. X-ray photoelectron spectroscopy (XPS) of A) 3R-MoS_2 (550˚C), 3R-MoS_2 (650˚C) and 3R-MoS_2 (750˚C), and B) 3R-WS_2 (550˚C), 3R-WS_2 (650˚C) and 3R-WS_2 (750˚C).

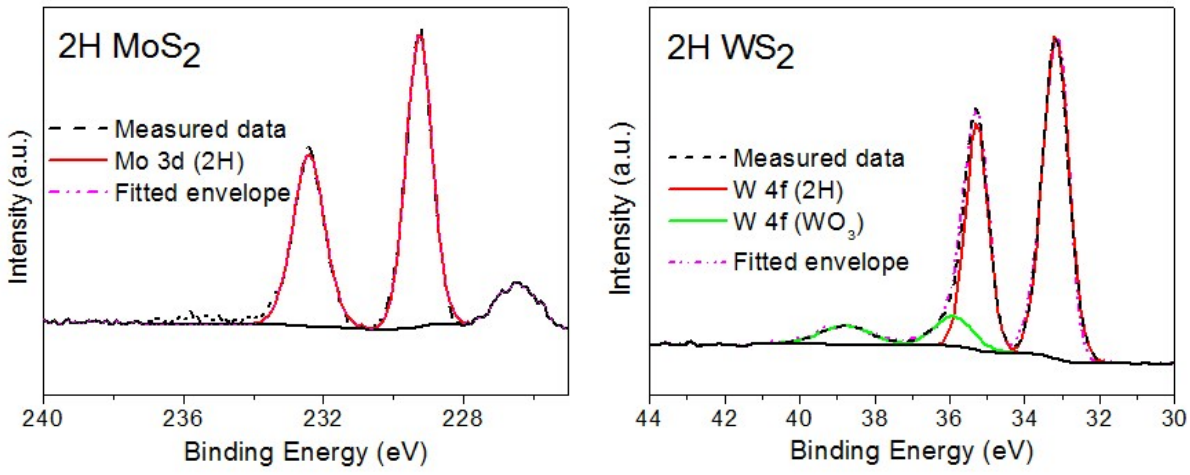

Figure S16. X-ray photoelectron spectroscopy (XPS) of 2H-MoS2 and 2H-WS2 single crystals.

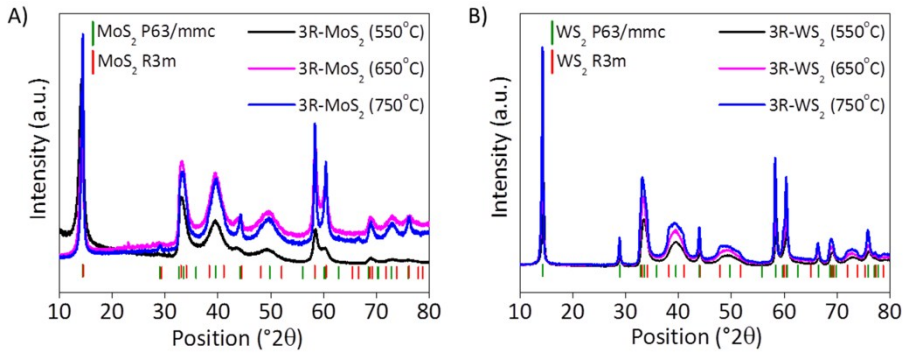

Figure S17. X-ray diffraction (XRD) patterns of A) 3R-MoS_2 (550˚C) (black line), 3R-MoS_2 (650˚C) (red line) and 3R-MoS_2 (750˚C) (blue line), and B) 3R-WS_2 (550˚C) (black line), 3R-WS_2 (650˚C) (red line) and 3R-WS_2 (750˚C) (blue line).

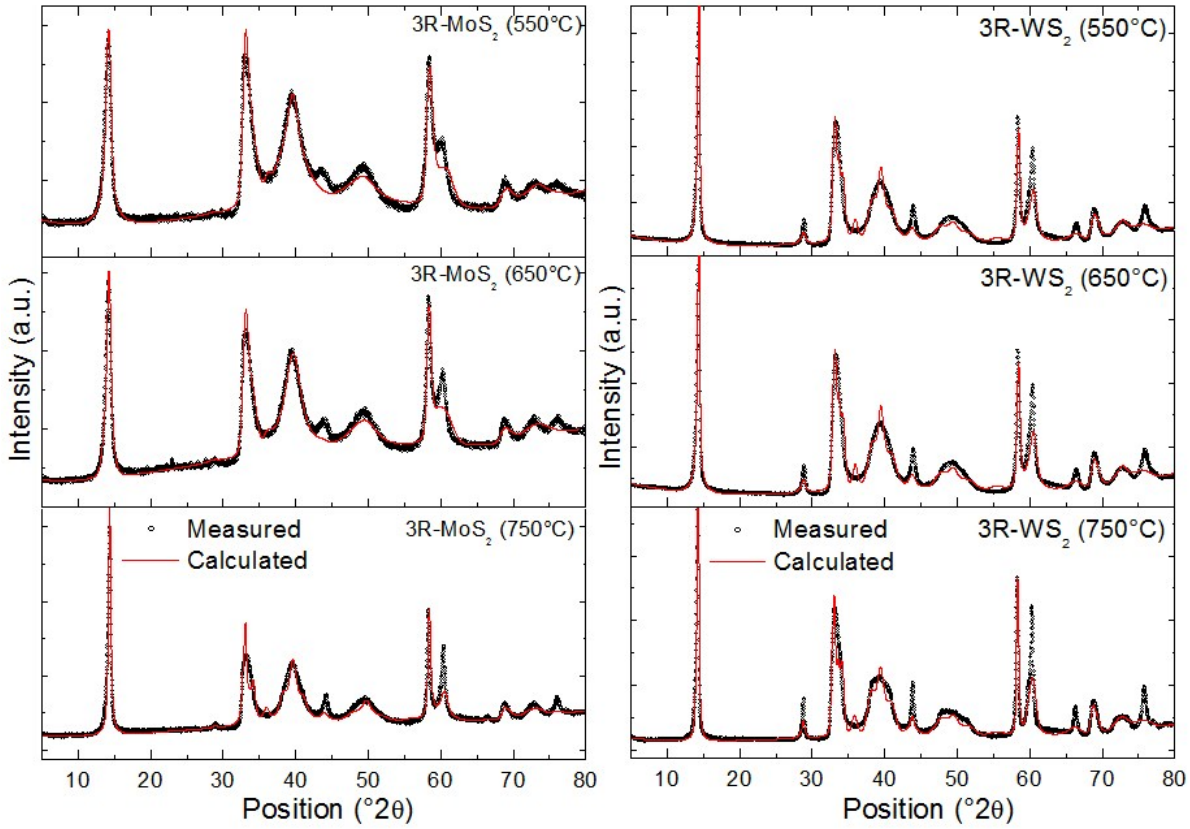

Figure S18. X-ray diffraction patterns and calculated profile obtained by Rietveld method used for phase composition calculation. 3R-MoS_2 (550°C) contain 28 wt.% 2H phase and 72 wt.% 3R phase, 3R-MoS_2 (650°C) contained 30 wt.% 2H phase and 70 wt.% 3R phase, and 3R-MoS_2 (750°C) contained 32 wt.% 2H phase and 68 wt.% 3R phase. 3R-WS_2 (550°C) contained 30 wt.% 2H phase and 70 wt.% 3R phase, 3R-WS_2 (650°C) contained 30 wt.% 2H phase and 70 wt.% 3R phase and 3R-WS_2 (750°C) contained 26 wt.% 2H phase and 74 wt.% 3R phase.

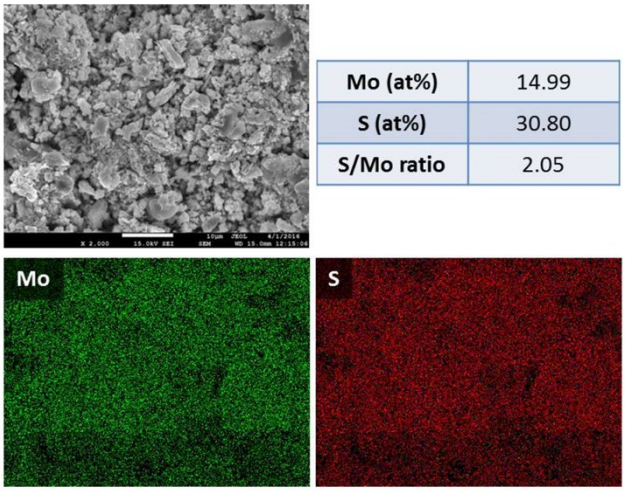

Mo (at%)	14.99
S (at%)	30.80
S/Mo ratio	2.05

Figure S19. Energy-dispersive X-ray spectroscopy (EDS) data for 3R-MoS_2 (650°C). Scale bar, 10 µm.

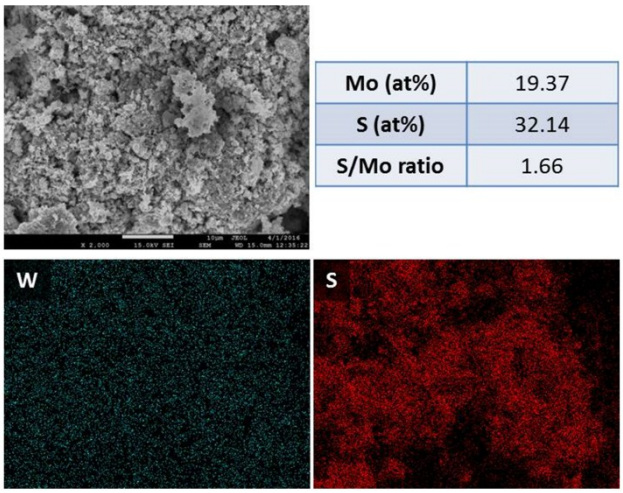

Mo (at%)	19.37
S (at%)	32.14
S/Mo ratio	1.66

Figure S20. Energy-dispersive X-ray spectroscopy (EDS) data for 3R-WS_2 (650˚C). Scale bar, 10 µm.

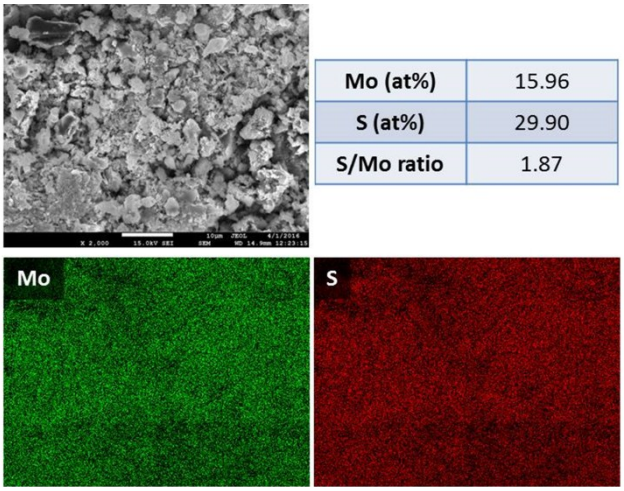

Mo (at%)	15.96
S (at%)	29.90
S/Mo ratio	1.87

Figure S21. Energy-dispersive X-ray spectroscopy (EDS) data for 3R-MoS_2 (750˚C). Scale bar, 10 µm.

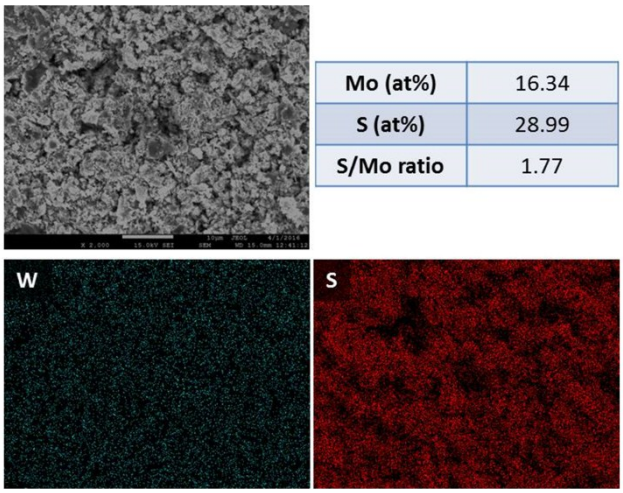

Mo (at%)	16.34
S (at%)	28.99
S/Mo ratio	1.77

Figure S22. Energy-dispersive X-ray spectroscopy (EDS) data for 3R-WS_2 (750˚C). Scale bar, 10 µm.

References:

[1] P.W. Stephens, Phenomenological model of anisotropic peak broadening in powder diffraction, J. Appl. Cryst., 1999, 32, 281-289.